High-temperature slurry erosion of vinylester matrix composites – The effect of test parameters

Essi Sarlin[1], Mari Lindgren[2], Reija Suihkonen[1], Sanna Siljander[1], Markus Kakkonen[1], Jyrki Vuorinen[1]

[1]*Tampere University of Technology, Department of Materials Science, P.O. Box 589, FI-33101 Tampere, Finland*
[2]*Outotec Research Center, P.O. Box 69, FI-28101 Pori, Finland*

ABSTRACT
Glass fibre (GF) reinforced vinylester composites (VE-FRP) are commonly used materials in hydrometallurgical reactors, the pulp and paper industry and waste water treatment plants, due to their excellent chemical resistance combined with good mechanical performance. In these applications, materials can be subjected to erosion, elevated temperatures (as high as 95°C) and various chemical environments. However, studies on the slurry erosion of vinylester-based composites at high temperatures have not yet been reported.

In this study, the erosion resistance of GF reinforced VE-FRP was investigated with a pilot-scale reactor. The effect of slurry concentration, erodent particle kinetic energy and slurry temperature were studied. The dominating wear mechanism was found to be abrasive wear. The VE-FRP structure was found to be prone to erosive turbulent flow and cavitation. Moreover, an increase in the erodent concentration of the slurry (10-20 wt.%) or in the total kinetic energy of the erodent particles (30-770 kJ) increased the wear rate of the material markedly (up to 6 times higher weight loss). However, the total effect of different interrelated parameters was found to be complex. Consequently, it is recommended that predictions of the erosion rate of VE-FRP components are based on tests carried out in conditions that simulate the actual service environment.

Keywords: vinylester, FRP, glass fibre, erosion, slurry
Correspondence to E. Sarlin (essi.sarlin@tut.fi)

1. INTRODUCTION

Glass fibre (GF) reinforced vinylester composites (VE-FRP) have excellent chemical resistance combined with good mechanical performance. Hence they are commonly used construction materials in the harsh chemical environments of the hydrometallurgical process industry, the pulp and paper industry and waste water treatment plants [1]. In the hydrometallurgical processing of metals, construction materials can be subjected to erosion, elevated temperatures (as high as 95°C), and various chemical environments, like sulphuric acid [2]. Thus mastering the erosion properties of GF-reinforced VE-FRPs at high temperatures is essential in optimizing the maintenance intervals of different FRP equipment. The avoidance of unnecessary process shutdowns would provide major operating cost savings. However, the slurry erosion behaviour of VE-FRPs has not been studied at elevated temperatures.

The complex composite structure consisting of matrix and reinforcement(s) and its anisotropic and viscoelastic nature make the study of the erosion behaviour of composites a challenge. The wear mechanisms that take place during polymer erosion depend highly on the polymer type. Brittle polymers are susceptible to crack formation and brittle fracture, ductile polymers to cutting and chip formation, and elastomers generally exhibit tearing and fatigue. Thus, the erosion behaviour of a wide range of fibre-reinforced polymer composites with different matrix materials has recently been evaluated. These include glass and carbon fibre reinforced epoxy [3-5], polyester [6-9], polyetheretherketone (PEEK) [10], polyetherimine (PEI) [11, 12] and polyphenylenesulphide (PPS) [13], to name a few. Typically, the effect of the reinforcement material, concentration, type and orientation as well as its adhesion to the matrix has been studied in these investigations.

Moreover, as many as 20 interrelated test parameter combinations affecting the erosion performance of composites can be established [14]. Typically, the effects of test temperature, particle velocity, impingement angle, erodent material and its size, shape and hardness are studied [14, 15]. For example, the effect of the

erodent particle size and velocity can be estimated with the aid of its kinetic energy E_k, which has a major role in the erosion behaviour of materials [16]. The kinetic energy of erodent particles can be estimated by Eq. 1 [16]:

$$E_k = \frac{2}{3}\rho\pi R^3 V_P^2 \quad (1)$$

where ρ is the density, R the radius and V_p the velocity of the solid particles. All in all, the numerous different parameter combinations make it difficult to compare results between different studies.

Stemming from the fact that there are several possible wear modes and mechanisms, many types of wear testing devices exist. Some standard methods are used to rank the wear resistance of different materials, whereas some methods attempt to simulate an actual service environment as closely as possible. The slurry pot test is a commonly used test method to determine the slurry erosion behaviour of different materials on laboratory scale. Slurry pots are simple and easy to operate and can be used in ranking materials based on their erosion resistance as well as to reveal the basic wear mechanisms of the erosion process for a certain material [17, 18]. Since the particle flow inside the slurry pot is complicated, it may be challenging to match the particle velocity and impingement angle with a certain, real-life application [18-21]. Therefore, to assess the erosion resistance of materials under hydrometallurgical leaching environments, the testing apparatus design has to resemble the actual application as closely as possible. Computational fluid dynamics (CFD) modelling together with in-situ particle velocity measurements are used to study and validate virtual models of slurry pots [22, 23]. CDF model of the test set-up was created and the results were utilized in assessing the flow pattern. However, in this paper, the standpoint is empirical.

This research paper studies the erosion of GF-reinforced VE-FRP using a new in-house constructed erosion test apparatus. The apparatus consists of a pilot-scale reactor where the samples are attached to the agitator blades. The design allows heating of the slurry and the use of acids but in this study only aqueous slurry was employed. The slurry temperature, rotation speed, erodent particle size and concentration were varied and the erosion rates of the VE-FRP samples were measured. The worn samples were characterized by scanning electron microscopy in order to evaluate the erosion mechanisms in these rather complicated, two-component composite structures. The results of this study will provide a reference point for the corresponding measurements from tests conducted in sulphuric acid, which will be reported separately.

2. EXPERIMENTAL DETAILS

2.1 Laminates

The tested vinylester composites were manufactured by hand laminating using epoxy vinylester resin (Derakane Momentum 411-350 supplied by Ashland), which is based on a bisphenol-A epoxy resin. It is generally used in applications where good resistance to acids, alkalis, bleaches and solvents are needed [24]. The laminates contained six layers of C-glass chopped strand mat with a nominal weight of 300 g/m^2 each and on both surfaces one layer of 30 g/m^2 C-glass mat. C-glass is typically used in the corrosion barrier layer which is subjected to both aggressive environment and wear. The structure of the laminates is equal to the corrosion-resistant layer generally used in the surfaces of FRP structures applied in acidic hydrometallurgical leaching environments. Because the function of the corrosion-resistant layer is to protect the structural layer from chemical attack, the mechanical properties of the laminate were not considered relevant. The laminates were post-cured for 4 hours at 80°C.

All samples were cut from one laminate and the density, the glass transition temperature and the hardness of the laminate were measured. The density was 1.1416 g/cm^3 and was measured with a Wallace electronic densimeter. The glass transition temperature (T_g) of the laminate was 116.8°C and was measured with a differential scanning calorimeter (DSC), Netzsch DSC 204 model under a nitrogen flow of 50 ml/min at a temperature range of 25–200°C, according to ISO 11357-1:2009. The Barcol hardness of the laminate was 39 ± 4 and it was measured with a Barber-Colman Impressor GYZJ-934-1 with 45 parallel measurements according to the standard ASTM D2583. The fibre fraction of the laminate was 39.7 wt.% and was estimated by means of a residual ash determination test. In this test, a small sample (weight of approximately 1 g) was cut from the laminate and its temperature was raised gradually to 600°C in an oven. After all the resin had burned away, the remaining ash was weighed and compared to the original weight.

The erosion test samples (size 35 mm x 35 mm) were water jet cut from the laminate and the cut edges of the samples were sealed with vinylester resin (Derakane 441 supplied by Ashland) in order to avoid excess water intake. To cure the Derakane 441 layer and to provide a moisture-independent reference state, the samples were placed in an oven (80°C) for 6 hours and then weighed. To further minimize the edge effects, the cut edges were covered with the sample holder, as demonstrated in Fig. 1b. Two to six parallel samples were tested, depending on the erosion test conditions. After the test, the worn samples were brushed with a soft cloth and cleaned in an ultrasonication bath for one hour to remove any erodent material attached to the sample surfaces and to minimize the amount of loose wear debris that would affect the weight loss determination. Finally, the samples were dried in an oven (6 hours at 80°C), weighed and the weight loss values for each sample were calculated. The wear surfaces were characterized with a scanning electron microscope (SEM; model Zeiss ULTRAplus) using an acceleration voltage of 10 kV. Prior to the SEM studies, the specimens were coated with a thin gold layer to avoid charging.

2.2 Test set-up

The erosion wear tests were done with a new in-house constructed erosion test apparatus (Fig. 1a). In this apparatus, the sample holder with the samples was attached to the rotating main shaft that is connected to the motor, located on the top of the lid. A maximum rotation speed of 7.2 m/s at the tip of the blade could be achieved. Four baffles on the inner sides of the reactor walls controlled the flow of the slurry and prevented the flocculation of the erodent on the reactor walls. The temperature of the slurry could be raised with the heating coils up to 95 °C. No cooling system was built into the system. The slurry temperature during the test was monitored continuously with thermocouples.

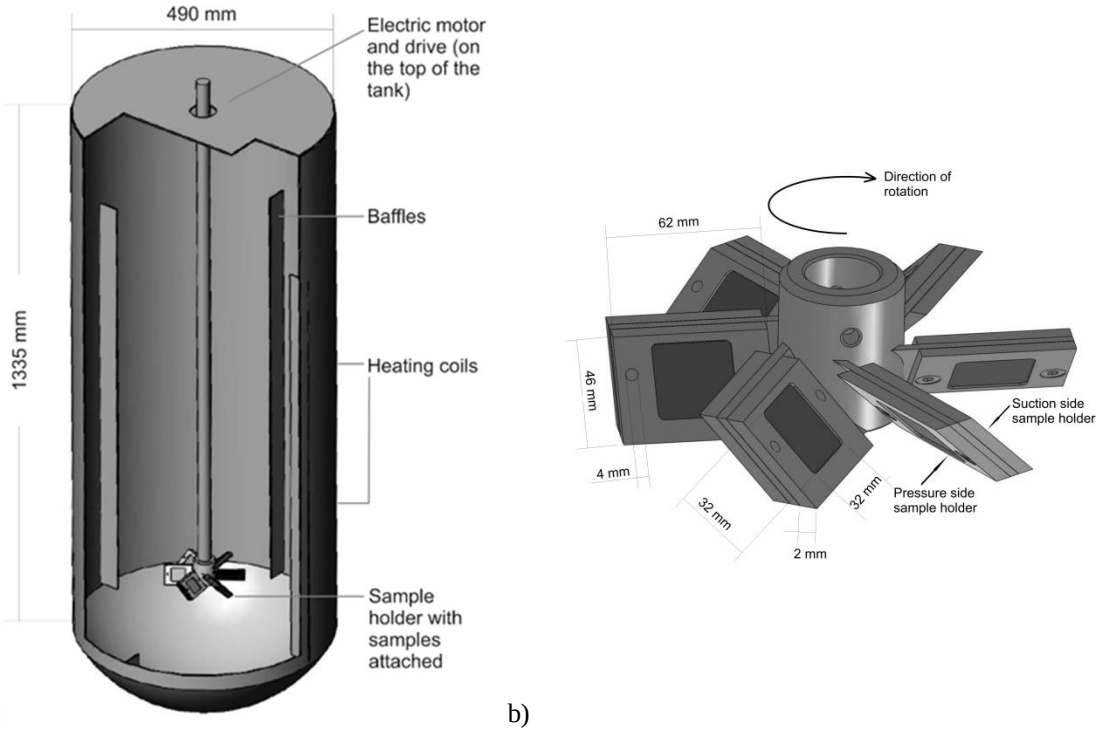

Figure 1: Schematic presentation of (a) the erosion test apparatus construction and (b) the agitator with the sample holders attached to its blades.

The sample holder in this test apparatus resembled one typical agitator type that is used in mixing solids with a liquid. Twelve samples could be tested at the same time and they were attached to the rotating agitator blades (fixed at 45° position), as illustrated in Fig. 1b. One half of the samples were on the pressure side and the second half on the suction side of the blades. It is known that during agitation a different pressure distribution is

generated in the pressure and suction sides of the agitator blades. Flow is more uniform on the pressure side of the blade [25, 26] although the velocity varies slightly (3.5 %) across the sample surface, due to the different local velocity of the blade. On the other hand, on the suction side of the blade, a trailing vortex is created leading to turbulent flow conditions and, consequently, to the localization of wear [22, 23].

In this study, an erodent concentration of 15 wt.% in the aqueous slurry was selected since it is typical for many hydrometallurgical processes. However, in order to study the effect of slurry concentration, tests were also conducted using concentrations of 10 wt.% and 20 wt.%. The slurry was assumed to be homogenous i.e. the concentration of the slurry was calculated based on the mass fractions of water and erodent. Justification for this was the absence of heavy sediment layer on bottom or walls of the erosion test apparatus. The tap water used is considered to be soft (water hardness < 5° dH). After each test, the slurry was pumped out, the reactor was washed and then filled with fresh tap water and new quartz sand because the wear rate is reduced when the particles get smaller and rounder. The rotation speed at the tip of the blade varied between 3.7 and 7.2 m/s. The speed at the tip of the blade was used as the particle velocity. Based on the computational fluid dynamics (CFD) modelling of the test set-up it can be estimated that the maximum particle impact velocity is somewhat less than the tip speed. However, since the CFD modelling alone do not provide reliable data either, the theoretical maximum value (tip speed) was used in the analysis. The test duration was 72 hours. The test parameters were selected to be typical for the hydrometallurgical process equipment.

The maximum long-term service temperature for the tested vinylester resin in such conditions is 80 °C, according to the supplier [24]. The maximum service temperature in this case is the highest known temperature at which equipment made with the resin has shown good service life in the industry or tested in the laboratory with results that indicate a good life expectancy in service [24]. However, since the activity of water is lower in sulphuric acid solutions [27], higher service temperatures can be achieved. In many hydrometallurgical applications, the process temperatures are above 80°C, generally close to 100°C. Therefore, it was crucial to study the VE-FRP wear loss at higher temperatures also. The slurry was heated to 80°C or 95°C, using two heating coils situated in the lower part of the reactor. The test temperature was achieved during the first four hours of the test. However, since there is no cooling system in the test equipment, the temperature of the 80°C tests continued to rise due to the frictional forces caused by the slurry agitation and the temperature of 95°C was reached after approximately two days of the three-day test. The test condition combinations are summarised in Table 1.

Table 1: The test matrix to study the effects of erodent concentration in the slurry, temperature and erodent particle kinetic energy (size and rotation speed) on the erosion behaviour of VE-FRP.

Slurry concentration (wt.%)	**Erodent particle size**	**Nominal slurry temperature (°C)**	**Rotation speed at the tip of the blade (m/s)**	**Test duration (h)**
10	Coarse quartz	80	4.8	72
15				
20				
15	Coarse quartz	80	4.8	72
		95		
15	Fine quartz	80	4.8	72
		95		
15	Coarse quartz	95	3.7	72
			4.8	
			7.2	

2.3 Erodent particles

Two erodents, fine and coarse quartz (both supplied by Sibelco Nordic Oy Ab), were investigated. The supplier provided a nominal particle size of 50-200 µm for the fine quartz and 100-600 µm for the coarse quartz. Prior to testing, the median values of the particle size distributions (P50) were measured by sieving and the specific

gravities were measured with a gas pycnometer (Table 2). The coarse quartz can be assumed to cause more erosion to VE-FRP, according to Eq. 1. The erodents were also characterized with a low vacuum scanning electron microscope (JEOL JSM-6490 LV). The SEM micrographs (Fig. 2) show that the shape of both quartz erodent particles was quite irregular and that the particles had sharp edges which can cause cutting and brittle fragmentation of the sample under erosion [15]. Since the quartz has relatively high Mohs hardness when compared to the raw materials generally used in mineral leaching processes and since it is generally accepted that the harder the erodent particle, the greater the erosion wear in the samples [28], quartz can be considered more destructive to the samples than most of the minerals used in actual processes.

Table 2: The properties of the used quartz erodents.

Sample	Nominal particle size (µm)	P50 (µm)	Density (g/cm^3)	Mohs hardness [29]
Coarse quartz	100-600	277	2.66	7
Fine quartz	50-200	121	2.70	

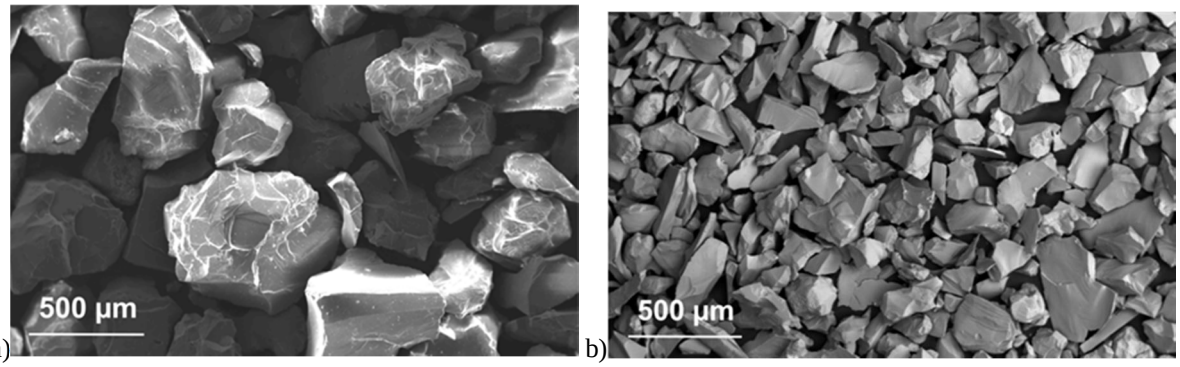

Figure 2: SEM images of the erodents: (a) coarse quartz and (b) fine quartz.

3. RESULTS AND DISCUSSION

3.1 Wear mechanism

The wear surfaces of VE-FRP samples indicated that the wear mechanism was mainly abrasive. It was seen that the erosion process started with the creation of microcracks in the matrix and continued with local matrix removal, which was seen as small notches, grooves and sharp dents in the worn surfaces. The sample surfaces were worn uniformly throughout the sample surface, except for the upper blade tip corner on the pressure side due to the locally higher sample velocity, and for the upper corner close to the axle on the suction side due to the vortex [20]. In these areas, more heavily worn areas were observed (see Section 3.2). The removal of the matrix revealed underlying glass fibres and fibre bundles, which were thus also exposed to the erodent particles. This induced fragmentation of the brittle fibres into small parts (Fig. 3a). When these parts were detached from the matrix, distinctive and deep tracks were left behind (Fig. 3a-b). This kind of brittle erosion behaviour of FRP materials has also been reported by other researchers [9-11, 14]. In addition, in some samples under specific test conditions, some of the revealed glass fibres were flattened, as shown in Fig. 3c. The reason for this is assumed to be the collapsing vapour cavities (cavitation) that were generated in the liquid at high temperatures and high rotation speeds [30]. Once the vapour cavities collapse, a very high pressure occurs locally and the fibres fracture in a brittle manner. In some samples, cavitation has caused the creation of spherical cavitation pits in the matrix with a diameter of 70-150 µm (Fig. 3d). The erosion due to cavitation was observed especially in the samples tested at high temperature and/or high rotation speed.

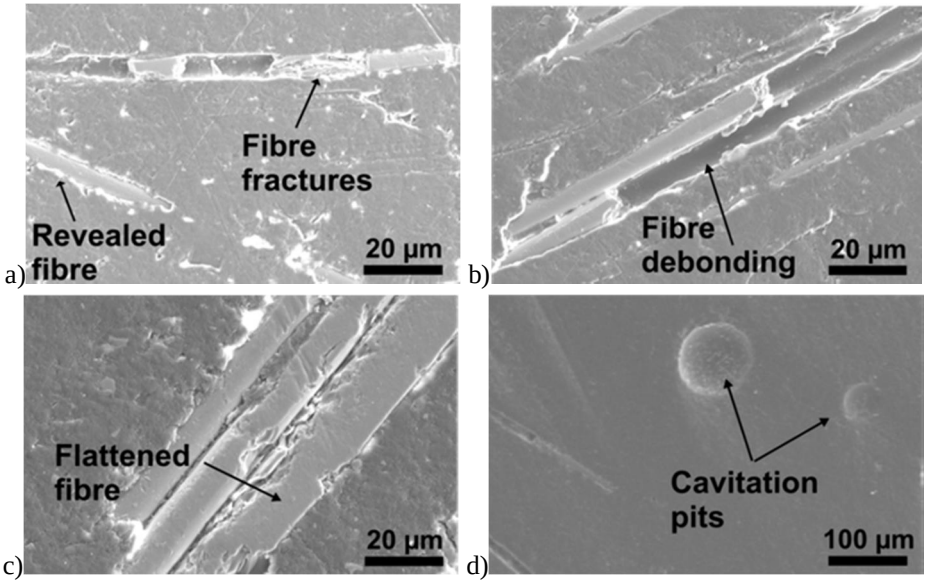

Figure 3: SEM images of the VE-FRP wear surfaces.

3.2 Comparison of pressure and suction side results

A visual inspection of the worn pressure and suction side sample surfaces showed that the crater due to localized wear was more extensive in the suction side samples, as demonstrated in Fig. 4. In both pressure and suction side samples, the location of the localized wear was in the upper part of the samples. On the pressure side it was in the blade tip corner where the sample velocity was slightly higher. In contrast, on the suction side samples, the locus of localized wear was in the corner closer to the axle i.e. on the edge with the lower tip speed. The craters in the suction side samples were also surrounded by several smaller pits and grooves. This kind of behaviour was clearly visible in all test conditions. The results agree with the known flow characteristics: on the pressure side the higher velocity of the slurry at the outer edge of the blade intensifies wear and on the suction side the vortex localises the wear [22, 23, 25, 26].

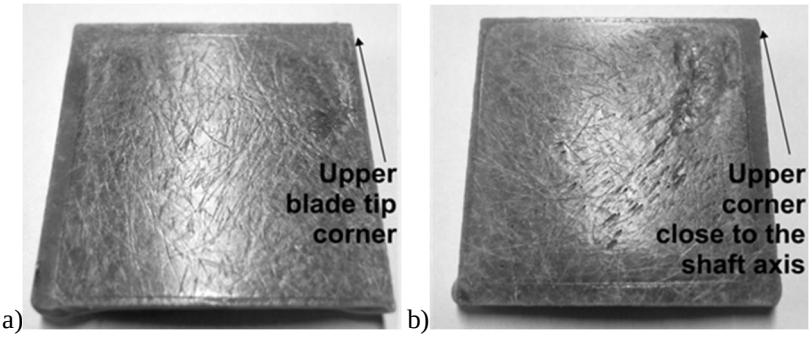

Figure 4: Typical wear patterns in (a) pressure side and (b) suction side samples (15 wt.% of coarse quartz at 80°C, 4.8 m/s, 72 h).

Generally, the weight loss of the pressure side samples was smaller than that of the suction side (Fig. 5), which is consistent with the visual inspection results. The weight loss of the pressure side samples was more sensitive to the changes in test conditions (except for the slurry concentration) than the suction side samples, whose weight loss was dominated by the heavy mass loss due to the trailing vortex. To study the significance of the obtained data, a linear regression analysis was done for the pressure and suction side data separately. The significance value F was 0.02 for both data sets, which indicates that the whole data set can be regarded as significant. The SEM images of the worn pressure and suction side sample surfaces (Fig. 6) clearly show the differences in the extent of wear rate. However, the actual wear mechanisms (abrasive wear) seemed to be the same on both sides. The pressure side samples exhibited wear surfaces where individual fibres or small fibre

bundles were revealed whereas the suction side samples displayed large areas of exposed fibres and fibre bundles inside and around the crater.

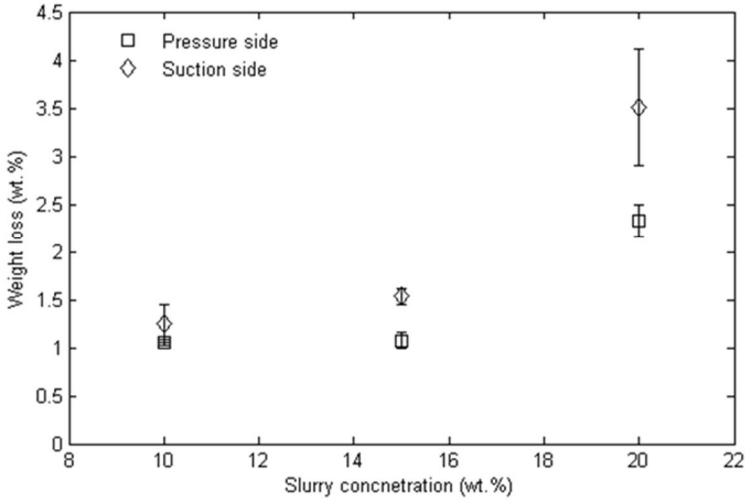

Figure 5: The effect of sample position (pressure or suction side) and erodent concentration in the slurry on the erosion weight loss of VE-FRP (coarse quartz at 80°C, 4.8 m/s, 72 h). The error bars describe the standard deviation of the results.

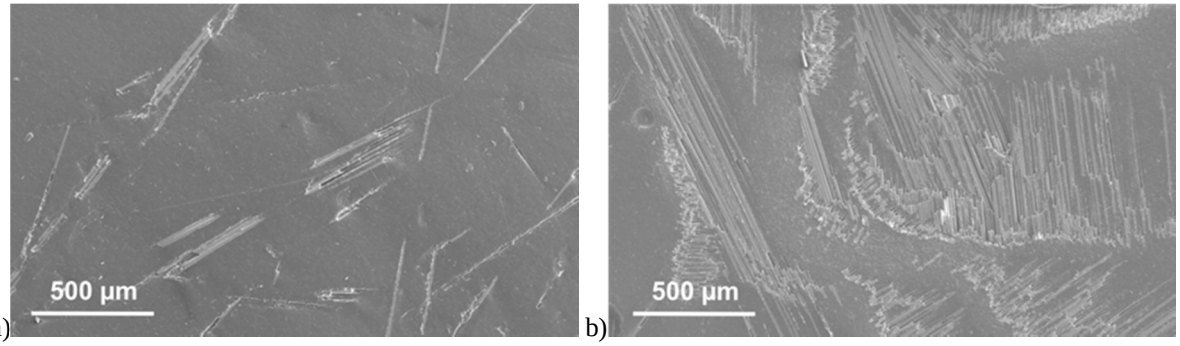

a) b)

Figure 6: SEM images on the wear surfaces in (a) pressure and (b) suction side samples (15 wt.% of coarse quartz at 80°C, 4.8 m/s, 72 h)

3.3 Effect of erodent concentration in the slurry

The average weight loss versus the erodent concentration and the corresponding standard deviations are shown in Fig. 5. The weight loss at 10 wt.% erodent concentration is the same on both sides and increases with increasing concentration on the suction side. A two-term power series ($y = ax^b + c$) was fitted to the weight loss data using the MATLAB curve fitting tool. The results are shown in Table 3 together with the sum of squares due to error (SSE), which measures the total deviation of the response values from the fit to the response values and the R-square, which measures how successful the fit is in explaining the variation of the data. The exponent of the suction side curve (b≈12) is markedly higher than the exponent of the pressure side curve (b≈7), indicating that the erosion wear in the suction side samples is more sensitive to changes in slurry concentration. This indicates that erosive turbulent flow is particularly harmful for VE-FRP samples. Also, due to the non-linear behaviour of the weight loss with increasing erodent concentration in the slurry, even small changes in the concentration can change the wear rate of the VE-FRP significantly. Consequently, this should be considered when evaluating the maintenance cycle or the lifetime of a VE-FRP component in erosive environments.

Table 3: The two term ($y = ax^b + c$) power series curve fitting results for the weight loss versus erodent concentration data.

	Pressure side	**Suction side**
a	$2.06 \cdot 10^{-9}$	$3.70 \cdot 10^{-16}$
b	6.95	11.94
c	1.22	1.04
SSE	$9.93 \cdot 10^{-11}$	$5.78 \cdot 10^{-5}$
R-square	1.00	1.00

When the weight loss results are analysed per unit erodent mass (Fig. 7), it can be seen that on the pressure side the weight loss per unit erodent mass can be considered nearly constant as a function of erodent concentration. On the suction side, an increasing trend can be observed under higher concentrations. This behaviour differs significantly from the behaviour of metallic materials, for which the weight loss per unit erodent mass tends to decrease with increasing concentration [31, 32]. For metals, the decreasing erosion rate is explained by the increasing degree of erodent particle-particle interaction, which lowers their kinetic energy below a threshold level under which only elastic deformation of the metal surface occurs [21]. Similarly, increasing particle-particle interaction and smaller kinetic energy was expected in the current tests. As the weight loss per unit erodent mass on the pressure side was constant as a function of slurry concentration, one can assume that there is no threshold level for kinetic energy to damage the VE-FRP surface. Thus, even particles with low kinetic energy can cause some degree of damage, probably due to the low hardness of the VE-FRP when compared to metallic materials. On the contrary, the increasing wear rate on the suction side may be due to the combined effect of increasing slurry concentration and the vortex: higher concentration increased the slurry viscosity and consequently enlarged the size of the trailing vortex, resulting in more significant erosion.

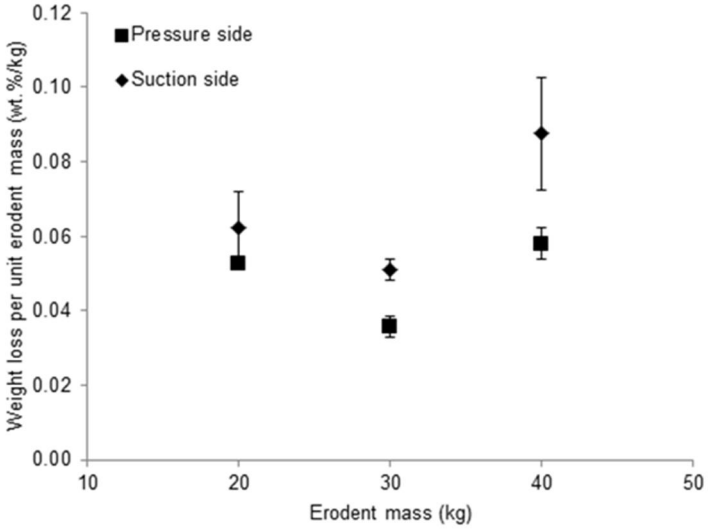

Figure 7: The weight loss of VE-FRP per unit erodent mass in pressure side and suction side. The error bars describe the standard deviation of the results.

Visual and SEM inspections were in line with the mass loss results: the concentration did not have any significant effect on the pressure side samples (Fig. 8) but, in the suction side samples, the crater size increased significantly with higher concentration (Fig. 9). A change in the erodent concentration from 10 wt.% to 15 wt.% increased the size of the suction side crater from 5 mm x 10 mm to roughly 5 mm x 15 mm. With a concentration of 20 wt.%, the crater widened (roughly 10 mm x 15 mm) and became deeper (depth more than 1 mm). Also, more grooves were observed close to the crater and the grooves became more diagonally oriented and deeper with increasing erodent concentration.

Figure 8: Typical wear patterns of the pressure side samples as a function of the erodent concentration: (a) 10 wt.%, (b) 15 wt.%, and (c) 20 wt.% (coarse quartz at 80°C, 4.8 m/s, 72 h).

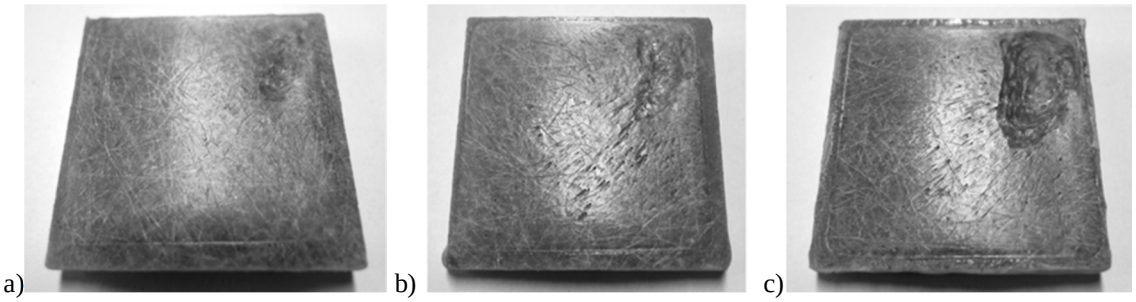

Figure 9: Typical wear patterns of the suction side samples as a function of the erodent concentration: (a) 10 wt.%, (b) 15 wt.%, and (c) 20 wt.% (coarse quartz at 80°C, 4.8 m/s, 72 h).

3.4 Effect of temperature

Visual inspection after the tests revealed that the samples were rather matte surfaced whereas the pristine samples were translucent. Further, the colour of the samples tested at 95°C was whiter than the samples tested at 80°C. Since the test laminate was post-cured at 80°C, some post-curing can be expected to occur during testing. To study the origin of the colour change, differential scanning calorimetry (DSC) tests were carried out. Samples cut from the bare laminate, as well as the samples sealed from the edges with vinylester, post-cured during the DCS test when tested, which indicates that the laminate was not fully cured before erosion testing after the initial post-curing. On the other hand, the DSC graphs of the erosion-tested samples did not show any signs of post-curing during the DSC test, which indicates that it had taken place during erosion testing. The colour difference between the samples tested at 80°C and 95°C can be explained by the hydrolytic degradation of vinylester matrix [33].

In the SEM investigation, the wear surfaces tested at higher temperatures showed more cavitation pits, as shown for the pressure side samples in Fig. 10, which was expected since the formation tendency of vapour cavities in a liquid grows with increasing temperature [30]. On the suction side, the vortex presumably induces even more vapour cavities and the wear is even more dominated by cavitation.

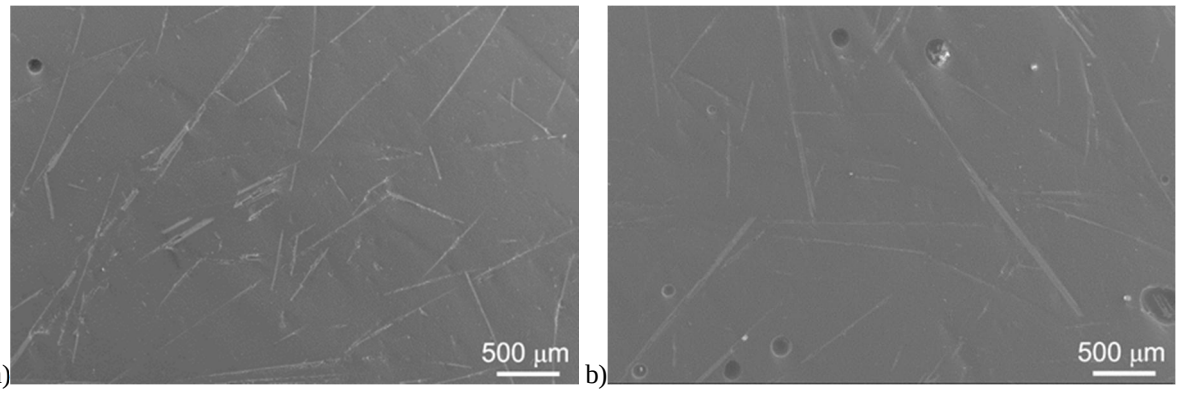

Figure 10: SEM images of the worn pressure side samples tested at (a) 80°C and (b) 95°C (15 wt.% of coarse quartz, 4.8 m/s, 72 h).

Increasing temperature resulted in a higher erosion rate for the VE-FRP samples, especially when the erodent was fine quartz (Fig. 11a). A higher erosion rate is to be expected due to the softening of the matrix at higher temperatures. Since the test parameters are interrelated, temperature change also induced changes to other test conditions. To study only the material behaviour of VE-FRP, AISI 316L stainless steel samples were also studied in corresponding conditions (Fig. 11b) [34]. The erosion rate of steel was lower at higher temperatures. Since the mechanical properties of steel do not change in the studied temperature range, the decreasing erosion rate is related to the increasing interaction between cavitation bubbles and erodent particles: a higher temperature induces more cavitation bubbles, which collide with quartz particles and decrease their energy. When the VE-FRP results are normalized with the AISI 316L results, the accelerating effect of temperature on VE-FRP erosion is even more noticeable. Thus, the loss of the mechanical properties of the vinylester matrix decreases the erosion resistance of VE-FRP samples at high temperatures.

The anomaly in the behaviour on the suction side at 95°C, where the increase in particle size leads to a decrease in erosion, can be understood when the presence of the trailing vortex is taken into account. Larger particles have higher kinetic energy, which tends to increase erosion. On the other hand, slurry consisting of larger particles has lower viscosity as a certain mass of the erodents is added. The lower viscosity generates a smaller trailing vortex, which consequently diminishes erosive wear on the suction side. These two factors tend to balance each other out. At 80°C, the effect of increasing kinetic energy dominated because an increase in weight loss was observed with the larger particles. In contrast, at 95°C, the formation of gas bubbles provides an additional factor because particle-gas interaction lowers the kinetic energy of the particles and may influence the properties of the trailing vortex. This additional factor accounts for the observation of lower erosion weight loss with larger particles at 95°C.

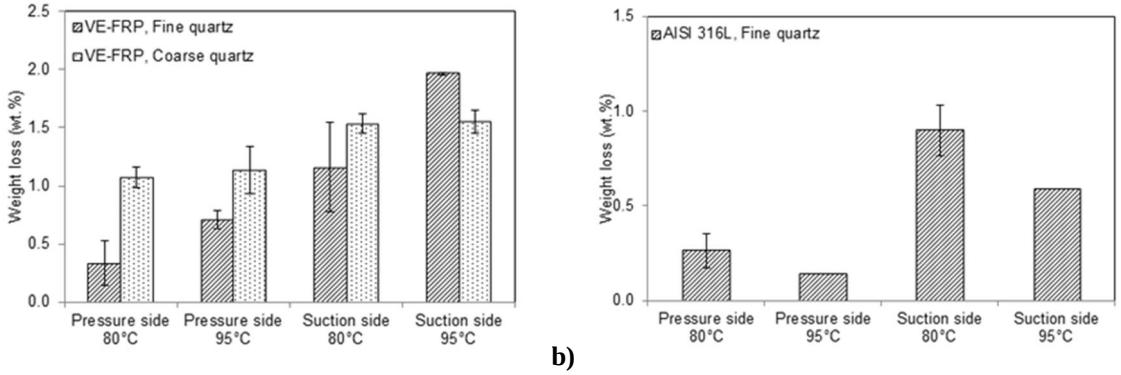

Figure 11: The effect of temperature on the weight loss for (a) VE-FRP and (b) stainless steel AISI 316L (15 wt.% of quartz, 4.8 m/s, 72 h). The error bars describe the standard deviation of the results.

3.5 Effect of erodent particle kinetic energy

To study the effect of the erodent particle kinetic energy on VE-FRP wear, both particle size and rotation speed were varied (see Table 1). Fig. 12 demonstrates that higher kinetic energy caused much higher weight losses on the pressure side, whereas on the suction side the weight loss did not show a clear dependency on the kinetic energy. On the pressure side, the effect of kinetic energy on weight loss was roughly linear, as expected according to Eq. 1. However, at very low kinetic energies, the curve does not begin from zero weight loss, so even low-energy particles are able to cause some weight loss in VE-FRP structures. This agrees with the results obtained when the effect of concentration was studied. The data points obtained by altering the particle size and velocity did not fall exactly on the same line. The most probable reason for this is the fact that the particle size used in the calculation of kinetic energy was the median size of the particle size distribution (half of the P50 value), which gave a very simplified measure of the particle size. On the suction side, there seemed to be no dependency between the measured weight loss and the kinetic energy of the particles. There are several contributing factors to the observed behaviour. A higher rotation speed increases the kinetic energy of the particles but at the same time allows samples to escape the trailing vortex more rapidly. Similarly, a higher rotation speed promotes the formation of cavitation pits but simultaneously, the interaction between particles and the gas phase may reduce the particle kinetic energy. These opposite trends counteract each other. To study the statistical significance of the data, linear regression analysis was done. For the pressure side, the significance value F was less than 0.01, so the data is good. However, at the suction side, the significance value F was too high due to the data points measured with the lowest erodent kinetic energy. This can be due to the factors of uncertainty discussed above.

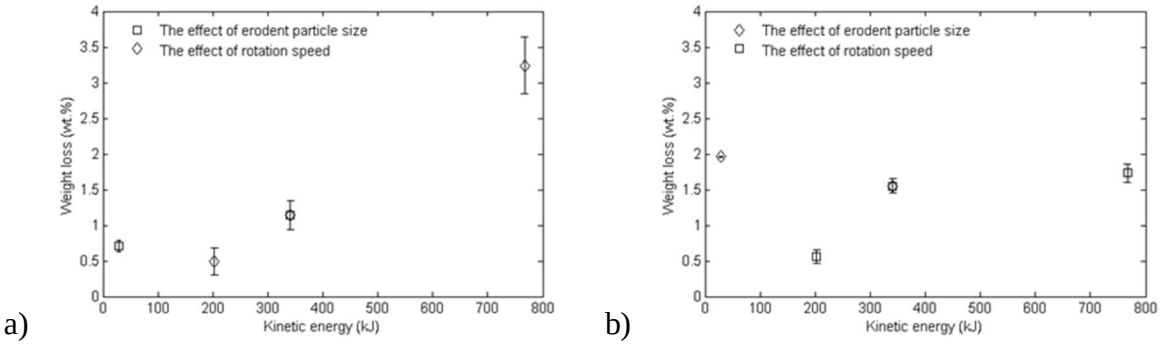

Figure 12: The effect of erodent particle kinetic energy on VE-FRP erosion for (a) pressure and (b) suction side samples (15 wt.% quartz at 95°C, 72 h). The error bars describe the standard deviation of the results.

The SEM images of the wear surfaces revealed that fine quartz caused less damage on the pressure side (Fig. 13a), while coarse quartz generated massive matrix removal and exposure of fibres and fibre bundles (Fig. 13b). Similar findings in terms of the effect of the particle size have also been reported by others [15]. It is generally accepted that the particle size increases the erosion wear until a certain limit is achieved [15, 21]. This limit is reported to be around 100-200 µm, but it is greatly affected by the test conditions and particle-target interaction [15]. In this study, both of the quartz sizes exceeded that limit, meaning that in the tested conditions the limiting particle size was higher.

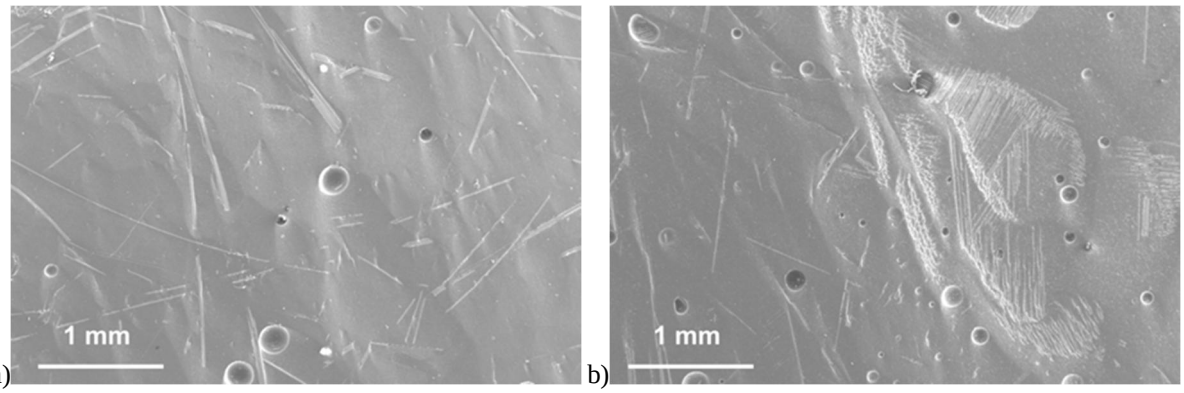

Figure 13: SEM images of the worn VE-FRP surfaces tested with (a) fine and (b) coarse quartz (pressure side samples, 15 wt.% of quartz at 95°C, 7.2 m/s, 72 h).

With increasing rotation speed, a more heavily worn area started to emerge, especially on the blade tip on the pressure side (right side of the samples in Fig. 14) where the rotation speed was higher. The amount of cavitation pits also increased with a rising rotation speed, which is to be expected since an increased rotation speed intensifies cavitation damage [35].

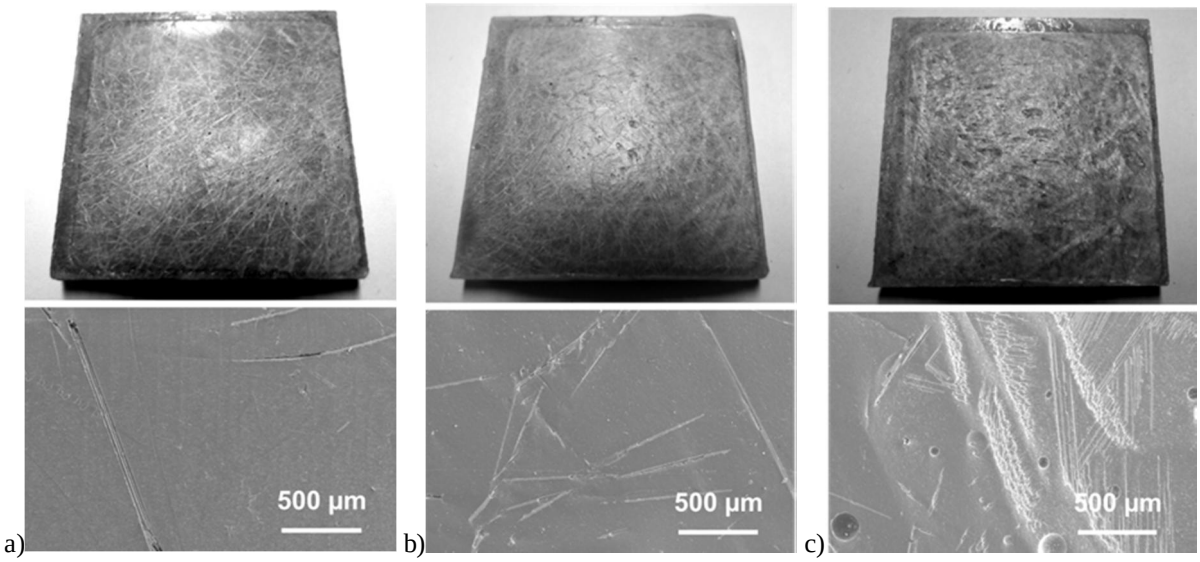

Figure 14: Photographs and SEM images from the blade tip of VE-FRP wear surfaces tested with (a) 3.7 m/s (b) 4.8 m/s, and (c) 7.2 m/s (pressure side, 15 wt.% of coarse quartz at 95°C, 72 h).

At a higher rotation speed, the wear mode was abrasive (Fig. 15b-c). However, with the lowest rotation speed, the worn matrix surface exhibited a rather fatigue-like wear mechanism (Fig. 15a). While small impingement angle particles at high speed cause abrasive wear, fatigue is more likely to occur if the impingement angle is high and the particle velocities are small [36]. At high rotation speeds, the slurry is more likely to follow the sample surface whereas at lower rotation speeds the probability of swirls and high-angle collisions grows. Thus a change in the wear mechanism is also to be expected. All in all, the rotation speed had many different effects on the erosion of VE-FRP: fatigue-like wear at low rotation speeds, abrasive-like wear at intermediate rotation speeds and the combined effect of cavitation and abrasive erosion at high rotation speeds. Thus, if an accelerated erosion test is used to evaluate the maintenance cycle or the lifetime of a composite structure, the actual wear mechanism of the material in the application has to be known and the test parameters have to be realistic. Otherwise, the conclusions may be unrealistic.

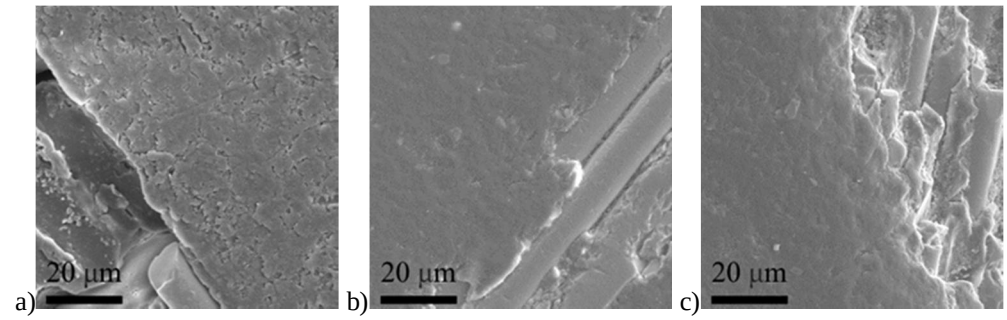

Figure 15: SEM micrographs from the matrix of worn VE-FRP surfaces with different rotation speeds: (a) 3.7 m/s (b) 4.8 m/s, and (c) 7.2 m/s (pressure side samples, 15 wt.% of coarse quartz at 95°C, 72 h).

4. CONCLUSIONS

Glass fibre (GF) reinforced vinylester composites (VE-FRP) are important construction materials in hydrometallurgical reactors due to their excellent chemical resistance and good mechanical performance. Inside the reactors, elevated temperatures (95°C) and erosive environments are present. In this study, the erosion resistance of GF-reinforced VE-FRP was investigated with a pilot-scale reactor. The effect of slurry concentration and temperature, as well as the erodent particle size and velocity were studied. In addition, the differences between the pressure and suction side samples were analysed.

The dominating wear mechanism was found to be abrasive wear, although at low rotation speeds the wear mode shifted towards fatigue-like wear and at high rotation speeds the cavitation erosion mechanism became more dominant. Therefore it must be emphasised that detailed knowledge of the actual service environment and flow conditions in the application is required before extrapolating any values from previous results. The VE-FRP structure was found to be prone to both erosive turbulent flow and cavitation. Moreover, even small changes in concentration can change the wear rate of the VE-FRP markedly. Consequently, this should be considered carefully when evaluating the maintenance cycle or the lifetime of a VE-FRP component in erosive environments.

The behaviour of VE-FRP was found to differ markedly from the behaviour of metals in corresponding conditions. Unlike metals, VE-FRP was also sensitive to the erodent concentration of the slurry at high concentrations and even low-energy particles caused this material to wear. All in all, the highly complex situation of the erosion test, where the parameters are interrelated, was found to cause sometimes unexpected total erosion mass losses. Consequently, it is emphasised that in order to predict the lifetime of VE-FRP components, tests should be carried out with a test set-up that resembles the actual application environment as well as possible.

Acknowledgements

The work has been done within the FIMECC LIGHT program funded by Finnish Funding Agency for Technology (Tekes) and the participating companies. The authors would like to thank Tekes for its financial support. Ms. Sinikka Pohjonen, M.Sc. Kosti Rämö, M.Sc. Eeva Hykkö and Ms. Meri Kiviniemi are also gratefully acknowledged for their help with the experiments.

References

[1] J. Graham, T. Johnson, D. Kelley, Optimum material solutions for industrial hydrometallurgical equipment, Proceedings of COM 2012, Niagara Falls, Canada, 30.9.2012-3.10.2012.

[2] H.R. Watling, Chalcopyrite hydrometallurgy at atmospheric pressure: 1. Review of acidic sulfate, sulfate–chloride and sulfate–nitrate process options, Hydrometallurgy 140 (2013) 163-180.

[3] A.P. Harsha, S.K. Jha, Erosive wear studies of epoxy-based composites at normal incidence, Wear 265 (2008) 1129–1135.

[4] V.K. Srivastava, A.G. Pawar, Solid particle erosion of glass fibre reinforced flyash filled epoxy resin composites, Compos. Sci. Technol. 66 (2006) 3021–3028.

[5] N.H. Yang, H. Nayeb-Hashemi, A. Vaziri, Non-destructive evaluation of erosion damage on E-glass/epoxy composites, Composites: Part A 39 (2008) 56–66.
[6] A. Patnaik, A. Satapathy, S.S. Mahapatra, R.R. Dash, A Taguchi approach for investigation of erosion of glass fiber-polyester composites, J. Reinf. Plast. Compos. 27 (2008) 871-888.
[7] A. Patnaik, A. Satapathy, S.S. Mahapatra, R.R. Dash, Optimization erosion wear of polyester-GF-alumina hybrid composites using the Taguchi method, J. Reinf. Plast. Compos. 27 (2008) 1039-1058.
[8] A. Patnaik, A. Satapathy, S. S. Mahapatra and R. R. Dash, Implementation of Taguchi design for erosion of fiber-reinforced polyester composite systems with SiC filler, J. Reinf. Plast. Compos. (2008), DOI: 10.1177/0731684407087688.
[9] K. Tsuda, M. Kubouchi, T. Sakai, A.H. Saputra, N. Mitomo, General method for predicting the sand erosion rate of GFRP, Wear 260 (2006) 1045–1052.
[10] G. Drensky, A. Hamed, W. Tabakoff, J. Abot, Experimental investigation of polymer matrix reinforced composite erosion characteristics, Wear 270 (2011) 146–151.
[11] R. Rattan and J. Bijwe, Carbon fabric reinforced polyetherimide composites: Influence of weave of fabric and processing parameters on performance properties and erosive wear, Mater. Sci. Eng., A 420 (2006) 342–350.
[12] S. Arjula, A.P. Harsha, and M.K. Ghosh, Erosive wear of unidirectional carbon fibre reinforced polyetherimide composite, Mater. Lett. 62 (2008) 3246–3249.
[13] T. Sinmazųelik, S. Fidan, V. Günay, Residual mechanical properties of carbon/polyphenylenesulphide composites after solid particle erosion, Mater. Des. 29 (2008) 1419–1426.
[14] A. Patnaik, A. Satapathy, N. Chand, N.M. Barkoula, S. Biswas, Solid particle erosion wear characteristics of fiber and particulate filled polymer composites: A review, Wear 268 (2010) 249–263.
[15] N.M. Barkoula, J. Karger-Kocsis, Review: Processes and influencing parameters of the solid particle erosion of polymers and their composites, J. Mater. Sci. 37 (2002) 3807-3820.
[16] R.J.K. Wood, The sand erosion performance of coatings, Mater. Des. 20 (1999) 179-191.
[17] J.B. Zu, I.M. Hutchings, and G.T. Burstein, Design of a slurry erosion test rig, Wear 140 (1990) 331-344
[18] B.W. Madsen, Measurement of erosion-corrosion synergism with a slurry wear test apparatus, Wear 123 (1988) 127-142.
[19] W. Tsai, J.A.C. Humhrey, I. Cornet, A.V. Levy, Experimental measurement of accelerated erosion in a slurry pot tester, Wear 68 (1981) 289-293.
[20] H. McI. Clark, Particle velocity and size effect in laboratory slurry erosion measurements or do you know what your particles are doing? Tribol. Int. 35 (2002) 617-624.
[21] H. McI. Clark, The influence of the flow field in slurry erosion, Wear 152 (1992) 223-240.
[22] Z. Doulgerakis, M. Yianneskis, A. Ducci, On the interaction of trailing and macro-instability vortices in a stirred vessel-enhanced energy levels and improved mixing potential, Chem. Eng. Res. Des. 87 (2009) 412-420.
[23] S. Roy, S. Acharya, M.D. Cloeter, Flow structure and the effect of macro-instabilities in a pitched-blade stirred tank, Chem. Eng. Sci. 65 (2010) 3009-3024.
[24] DerakaneTM epoxy vinyl ester resins – Chemical resistance guide, Datasheet, Ashland.
[25] K.C. Kee, C.D. Rielly, measurement of particle impact frequencies and velocities on impeller blades in a mixing tank, Chem. Eng. Res. Des. 82 (2004) 1237-1249.
[26] T. Kumaresan, J.B. Joshi, Effect of impeller design on the flow pattern and mixing in stirred tanks, Chem. Eng. J. 115 (2006) 173-193.
[27] R.H. Perry, D.W. Green, Perry's chemical engineers' handbook, seventh ed., McGraw-Hill, New York, 1997.
[28] S. Arjula, A.P. Harsha, Study of erosion efficiency of polymers and polymer composites, Polym. Test. 25 (2006) 188–196.
[29] F.G.H. Blyth, M.H. de Freitas (ed.), A geology for engineers, seventh ed., Taylor & Francis, Amsterdam, 1984, pp. 61-81.
[30] J.-P. Franc, J.-M. Michel, Fundamentals of cavitation, Kluwer Academic Publishers, Dordrecht, 2004.
[31] G.R. Desale, B.K. Gandhi, S.C. Jain, Slurry erosion of ductile materials under normal impact condition, Wear 264 (2008) 322–330.
[32] S. Turenne, M. Fiset, J. Masounave, The effect of sand concentration on the erosion of materials by a slurry jet, Wear 133 (1989) 95-106.

[33] A. M. Visco, V. Brancato, N. Campo, Degradation effects in polyester and vinyl ester resins induced by accelerated ageing in seawater, Journal of Composite Materials 46(17) (2011) 2025-2040.
[34] M. Lindgren, R. Suihkonen, J. Vuorinen, Erosion wear of various stainless steel grades as impeller blade materials in high temperature aqueous slurry, accepted for publication in Wear.
[35] J.S. Carlton, Propeller design, in: J.S. Carlton (ed.), Marine propellers and propulsion, third ed., Butterworth-Heinemann, Oxford, 2012, p. 448.
[36] Abrasive, erosive and cavitation wear, in G. W. Stachowiak, A. W. Batchelor (Eds.), Engineering tribology, fourth ed., Butterworth-Heinemann, Oxford, 2014, pp. 525-576.

Corrigendum

Corrigendum to High-temperature slurry erosion of vinylester matrix composites – The effect of test parameters

Wear 328-329 (2015) 488–497

Essi Sarlin[a], Mari Lindgren[b], Reija Suihkonen[a], Sanna Siljander[a], Markus Kakkonen[a], Jyrki Vuorinen[a]

[a]Tampere University of Technology, Department of Materials Science, P.O. Box 589, FI-33101 Tampere, Finland
[b]Outotec Research Center, P.O. Box 69, FI-28101 Pori, Finland

---

The authors regret the mistake in the x-axis label of the Figure 12. Below, the x-axis labels have been revised.

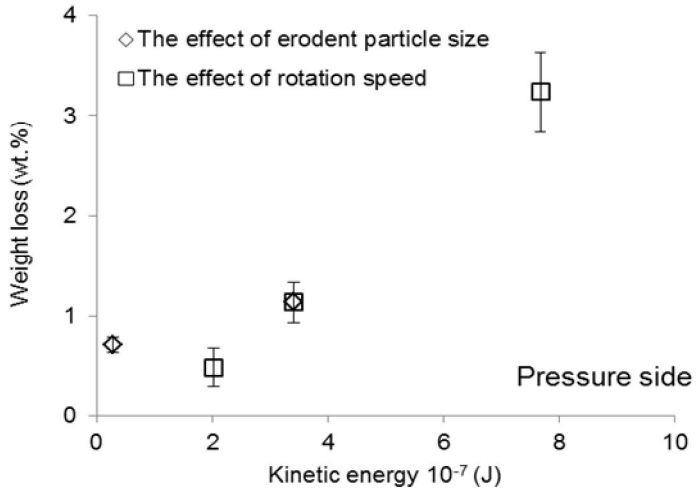

a)

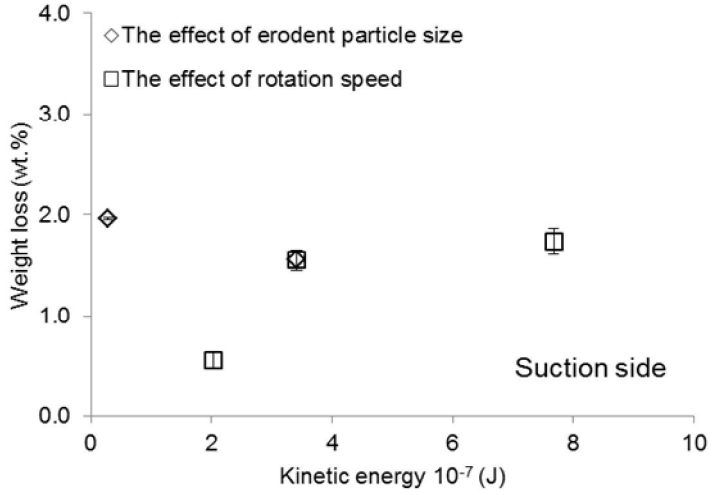

b)

Figure 12: The effect of erodent particle kinetic energy on VE-FRP erosion for (a) pressure and (b) suction side samples (15 wt% quartz at 95 °C, 72 h). The error bars describe the standard deviation of the results.

The authors would like to apologise for any inconvenience caused.

DOI of original article: 10.1016/j.wear.2015.03.021
Essi Sarlin
essi.sarlin@tut.fi